

Radiation absorption and Aligned Magnetic Field effects on MHD Dissipative fluid past an inclined vertical porous plate in Porous media

*Dr.B. Vishali¹,Dr.A.Haritha²,Dr.Y.Devasena³

¹Assistant Professor, Department of Applied Mathematics, Sri Padmavati Mahila Visvavidyalayam, Tirupati, A.P, India.

²Assistant Professor, Department of BS&H, SoET, Sri Padmavati Mahila Visvavidyalayam, Tirupati, A.P, India.

³Assistant Professor, Department of BS&H, SoET, Sri Padmavati Mahila Visvavidyalayam, Tirupati, A.P, India.

Corresponding Author: *B. Vishali

Received: 29-06-2024

Revised: 22-07-2024

Accepted: 20-08-2024

Published: 27-08-2024

Abstract:

In this article, in the presence of the aligned magnetic field, chemical reaction, and radiation absorption results, the research centered on the analysis-free convective flow of a viscous, incompressible, and electrically conducting fluid via an inclined plate through a porous medium. The free stream velocity could obey exponentially increasing small disruption law. Analytically, two-term harmonic and non-harmonic functions overcome non-dimensional governing equations. Distributions of velocity, temperature, and concentration are explored in depth by graphs for different parameter values entering the problem. The skin friction coefficient, heat transfer rate, and mass transfer rate are derived. This research is useful in the steel industry monitoring molten iron flow, nuclear plant liquid metal cooling, and meteorology.

Keywords: Aligned magnetic field, Radiation absorption, MHD, Porous medium, Inclined angle, mixed convective flow.

I. INTRODUCTION

The phenomenon of free convection and mass movement flow of an electrically conducting fluid past an inclined heated surface under the effect of a magnetic field has drawn attention in its application to geophysics, astrophysics and many engineering problems such as cooling of nuclear reactors, aerodynamic boundary layer regulation and cooling towers. Mass transfer is one of the commonly observed phenomena of both chemical and biological sciences. As the fluid is at rest, the mass transfer occurs; mass is transmitted solely through molecular diffusion arising from gradients of concentration. Convective heat and mass transfer mechanism are identical in design with the limited concentration of group in fluid and higher mass transfer speeds. Several studies have also been carried out of simultaneous heat and mass transfer, assuming different physical conditions. In specific chemical engineering methods, the chemical reaction between a foreign mass and the fluid in which the plate lies happens. These processes exist in various industrial applications, including polymer manufacturing, ceramics or glassware processing, and food procession. Mohammed Ibrahim[1] analysed a two-dimensional unstable

Raghunath et al.[10] introduced Hall Effects on MHD Convective Rotating Flow across Endless Vertical Plate Past Porous Medium. Raghunath et al.[12] presented Heat and Mass

Movement of a Visco-Elastic Fluid Past Endless Vertical Oscillating Porous Plate Suresh Babu G et al.[13] mentioned Free Convection Heat Transfer Flow Study in a Vertical Conical Annular Porous Media. Nagendra Prasad et al.[14] studied Visco-elastic fluid MHD flow over an unbounded, rotating porous plate with the heat source and chemical reaction.

Our research focuses on the impact of introducing a second fluid on mixed convection flow. Orphan Aydm et al.[15] had an MHD mixed heat transfer flow across an inclined plate. Reddy et al. researched thermal diffusion and homogeneous chemical reaction results on MHD mixed convection flow with Ohmic heating[16]. Reddy et al. explored unstable MHD radiative, and chemical-reactive natural convection flows near a moving porous plate through a porous medium[17]. Raju et al.[18] considered MHD convective and dissipative fluid flow over porous medium in a flat channel with an isolated and impermeable bottom wall in Joule heating. Ravikumar et al.[19] addressed the combined results of a non-Newtonian fluid's heat absorption and magnet convective movement, namely, Rivlin-Ericksen movement past a semi-infinite vertical porous layer. Raju et al.[20] performed exact solutions for MHD-free convective boundary layer flow past a porous vertical surface in the presence of chemical reaction, thermal radiation, and suction.

In the context of an aligned magnetic field, chemical reaction and radiation absorption results, this analysis focuses on researching the free convective movement of a viscous, incompressible and electrically conducting fluid past an inclined plate via a porous medium. The freestream velocity could obey exponentially increasing small disruption law. Analytically, two-term harmonic and non-harmonic functions overcome non-dimensional governing equations. Distributions of velocity, temperature, and concentration are explored in depth by graphs for different parameter values entering the problem. Skin friction coefficient, heat transfer rate, and mass transfer rate are derived.

II . PHYSICAL AND STATISTICAL FORMULATION

Consider laminar, incompressible, viscous, electrically conducting and heat-absorbing fluid two-dimensional flow past an inclined plate inserted in a porous medium in the presence of chemical reaction and Dufour results. The flow is believed to be in the x -direction, taken around the semi-infinite inclined plate and standard y -axis. A magnetic field of uniform intensity B_0 is added at flow path angle α . Free stream velocity meets exponentially increasing small disruption law.

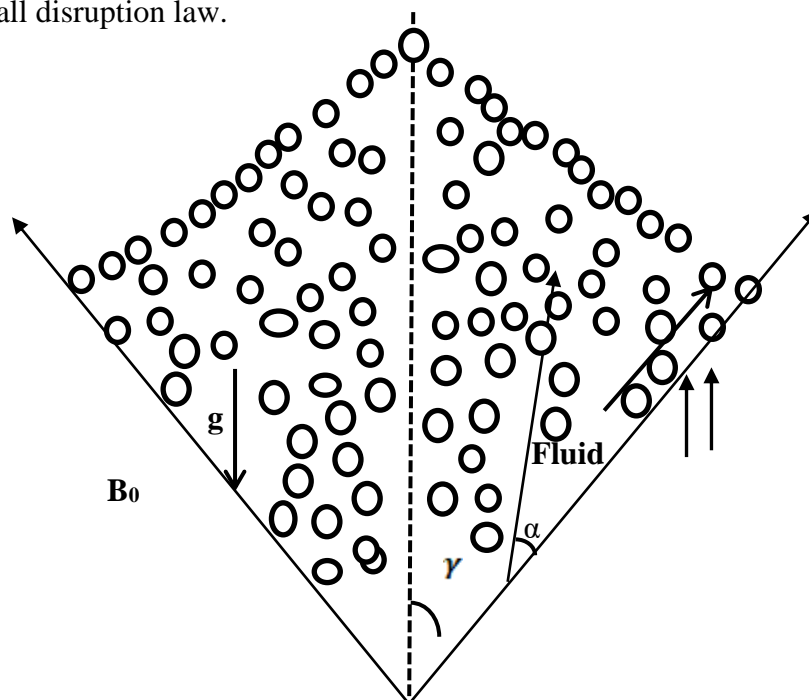


Figure 1: Physical problem-setting

The governing equations for this investigation are focused on mass, linear momentum, energy and concentration species equilibrium.

$$\frac{\partial v^*}{\partial y^*} = 0 \rightarrow v^* = -v_0 (v_0 > 0) \quad (1)$$

$$v^* \frac{\partial u^*}{\partial y^*} = \mathcal{G} \frac{\partial^2 u^*}{\partial y^{*2}} + g\beta(T^* - T_\infty) \cos \alpha + gB^*(C^* - C_\infty) \cos \alpha - \frac{\sigma B_0^2}{\rho} \text{Sin}^2 \gamma u^* - \frac{\mathcal{G} u^*}{k^*} \quad (2)$$

$$v^* \frac{\partial T^*}{\partial y^*} = \frac{k}{\rho C_p} \frac{\partial^2 T^*}{\partial y^{*2}} + \frac{\mathcal{G}}{C_p} \left(\frac{\partial u^*}{\partial y^*} \right)^2 + \frac{\sigma B_0^2}{\rho} u^{*2} + \frac{Q_0}{\rho C_p} (T^* - T_\infty) + \frac{R^*}{\rho C_p} (C^* - C_\infty) \quad (3)$$

$$v^* \frac{\partial C^*}{\partial y^*} = D \frac{\partial^2 C^*}{\partial y^{*2}} + -K_1 (C^* - C_\infty) \quad (4)$$

The appropriate boundary conditions for the corresponding fields are

$$\begin{aligned} u^* = 0 \quad T^* = T_w, \quad C^* = C_w \quad \text{at } y^* = 0 \\ u^* \rightarrow 0, \quad T^* \rightarrow T_\infty \quad C^* \rightarrow C_\infty \quad \text{as } y^* \rightarrow \infty \end{aligned} \quad (5)$$

Introduction of non-dimensional numbers,

$$\begin{aligned} u = \frac{u^*}{v_0}, \quad y = \frac{v_0 y^*}{\mathcal{G}}, \quad \text{Pr} = \frac{\mathcal{G} \rho C_p}{k}, \quad \theta = \frac{T^* - T_\infty}{T_w - T_\infty}, \quad \varphi = \frac{C^* - C_\infty}{C_w - C_\infty}, \quad \text{Gr} = \frac{\mathcal{G} g \beta (T_w - T_\infty)}{v_0^3}, \\ \text{Gm} = \frac{\mathcal{G} g \beta_c (C_w - C_\infty)}{v_0^3}, \quad \text{Ec} = \frac{v_0^2}{C_p (T_w - T_\infty)}, \quad M^2 = \frac{\sigma B_0^2 \mathcal{G}}{\rho v_0^2}, \quad k^* = \frac{\mathcal{G}^2}{K_0 v_0^2}, \quad \mathcal{G} = \frac{\mu}{\rho}, \quad \text{Sc} = \frac{\mathcal{G}}{D} \end{aligned} \quad (6)$$

$$S_0 = \frac{D_1 (T_w - T_\infty)}{\mathcal{G} (C_w - C_\infty)}, \quad \text{Kr} = \frac{\mathcal{G} K_1}{v_0^2}, \quad Q = \frac{Q_0 \mathcal{G}}{\rho C_p v_0^2}, \quad R = \frac{R^* \mathcal{G}^2 (C_w - C_\infty)}{k v_0 (T_w - T_\infty)}$$

Where Gr is the Grashof number, Gm is the Grashof number, Pr is the Prandtl number, Sc is the Schmidt number, Ec is the Eckert number, M is the magnetic parameter, Ko is the porous medium and Kr is the chemical reaction parameter.

The simple field EQs (2)-(4) may be represented as non-dimensional.

$$\frac{\partial u^2}{\partial y^2} + \frac{\partial u}{\partial y} - (M^2 \text{Sin}^2 \gamma + K_0) u = -G_r \cos \alpha \theta - G_m \cos \alpha \varphi \quad (7)$$

$$\frac{\partial^2 \theta}{\partial y^2} + \text{Pr} \frac{\partial \theta}{\partial t} + \text{Pr} \text{Ec} \left(\frac{\partial u}{\partial y} \right)^2 + \text{Pr} \text{Ec} M^2 u^2 + \text{Pr} Q \theta + R \varphi = 0 \quad (8)$$

$$\text{Sc} \frac{\partial^2 \varphi}{\partial y^2} + \frac{\partial \varphi}{\partial t} - \text{Kr} \varphi = 0 \quad (9)$$

The corresponding boundary conditions in dimensionless form are reduced to

$$\begin{aligned} \text{At } y^* = 0, \quad u = 0, \quad \theta = 1, \quad \varphi = 1 \\ \text{As } y^* \rightarrow \infty, \quad u \rightarrow 0, \quad \theta \rightarrow 1, \quad \varphi \rightarrow 1 \end{aligned} \quad (10)$$

Equations (7) – (9) describe a series of partial differential equations that can not be closed. However, it can be reduced to a series of regular, dimensionless differential equations that can be solved analytically. This can be achieved by reflecting tempo, temperature, and concentration.

$$\begin{aligned}
u(y,t) &= u_0(y) + E_c u_1(y) + O(Ec^2) \\
\theta(y,t) &= \theta_0(y) + E_c \theta_1(y) + O(Ec^2) \\
\phi(y,t) &= \phi_0(y) + E_c \phi_1(y) + O(Ec^2)
\end{aligned} \tag{11}$$

Using Equation (11) in Equations (7)–(9) and equating E_c 's similar power coefficient Zero order terms:

$$u_0'' + u_0' - (M^2 \sin^2 \gamma + K_0) u_0 = -Gr \cos \alpha \theta_0 - Gm \cos \alpha \phi_0 \tag{12}$$

$$\theta_0'' + Pr \theta_0' + Pr Q \theta_0 + R \phi_0 = 0 \tag{13}$$

$$Sc \phi_0'' + \phi_0' - Kr \phi_0 = 0 \tag{14}$$

First order terms:

$$\begin{aligned}
u_1'' + u_1' - (M^2 \sin^2 \gamma + K_0) u_1 &= -Gr \cos \alpha \theta_1 - Gm \cos \alpha \phi_1 \\
\theta_1'' + Pr \theta_1' + Pr Q \theta_1 &= -Pr (u_0')^2 - Pr M^2 u_0^2 - R \phi_1
\end{aligned} \tag{16}$$

$$Sc \phi_1'' + \phi_1' - Kr \phi_1 = 0 \tag{17}$$

Appropriate boundary conditions

$$\begin{aligned}
u_0 = 0, u_1 = 0, \theta_0 = 1, \theta_1 = 0, \phi_0 = 1, \phi_1 = 0 & \quad \text{at } y = 0 \\
u_0 \rightarrow 0, u_1 \rightarrow 0, \theta_0 \rightarrow 0, \theta_1 \rightarrow 0, \phi_0 \rightarrow 0, \phi_1 \rightarrow 0 & \quad \text{as } y \rightarrow \infty
\end{aligned} \tag{18}$$

Solving equations (14) – (19) under the boundary conditions (20), the following solutions are obtained

$$\theta_0 = b_1 \exp(-m_1 y) + b_2 \exp(-m_2 y) \tag{19}$$

$$\phi_0 = \exp(-m_1 y) \tag{20}$$

$$u_0 = b_3 \exp(-m_1 y) + b_4 \exp(-m_2 y) + b_5 \exp(-m_3 y) \tag{21}$$

$$\begin{aligned}
\theta_1 = b_6 \exp(-2m_1 y) + b_7 \exp(-2m_2 y) + b_8 \exp(-2m_3 y) + b_9 \exp(-(m_1 + m_2) y) + \\
b_{10} \exp(-(m_3 + m_2) y) + b_{11} \exp(-(m_1 + m_3) y) + b_{12} \exp(-m_5 y)
\end{aligned} \tag{22}$$

$$\phi_1 = 0 \tag{23}$$

$$\begin{aligned}
u_1 = b_{13} \exp(-2m_1 y) + b_{14} \exp(-2m_2 y) + b_{15} \exp(-2m_3 y) + b_{16} \exp(-(m_1 + m_2) y) + \\
b_{17} \exp(-(m_3 + m_2) y) + b_{18} \exp(-(m_1 + m_3) y) + b_{19} \exp(-m_5 y) + b_{20} \exp(-m_6 y)
\end{aligned} \tag{24}$$

The following solutions are obtained under boundary conditions (14) – (19) the velocity, temperature and concentration distribution in the boundary layer as follows

$$\begin{aligned}
u(y,t) = b_3 \exp(-m_1 y) + b_4 \exp(-m_2 y) + b_5 \exp(-m_3 y) + E_c [b_{13} \exp(-2m_1 y) + b_{14} \exp(-2m_2 y) \\
+ b_{15} \exp(-2m_3 y) + b_{16} \exp(-(m_1 + m_2) y) + b_{17} \exp(-(m_3 + m_2) y) + \\
b_{18} \exp(-(m_1 + m_3) y) + b_{19} \exp(-m_5 y) + b_{20} \exp(-m_6 y)]
\end{aligned} \tag{25}$$

$$\begin{aligned}
\theta(y,t) = b_1 \exp(-m_1 y) + b_2 \exp(-m_2 y) + E_c [b_6 \exp(-2m_1 y) + b_7 \exp(-2m_2 y) + b_8 \exp(-2m_3 y) + \\
b_9 \exp(-(m_1 + m_2) y) + b_{10} \exp(-(m_3 + m_2) y) + b_{11} \exp(-(m_1 + m_3) y) + b_{12} \exp(-m_5 y)]
\end{aligned} \tag{26}$$

$$\phi(y,t) = \exp(-m_1 y) \tag{27}$$

Skin Friction:

The surface's non-dimensional skin friction

$$\tau = \left(\frac{\partial u}{\partial y} \right)_{y=0} = \left(\frac{\partial u_0}{\partial y} \right)_{y=0} + E_c \left(\frac{\partial u_1}{\partial y} \right)_{y=0}$$

$$\tau = -(b_3 m_1 + b_4 m_2 + b_{13} m_3) - E_c [2b_{13} m_1 + 2b_{14} m_2 + 2b_{15} m_3 + b_{16} (m_1 + m_2) + b_{17} (m_3 + m_2) + b_{18} (m_1 + m_3) + b_{19} m_5 + b_{20} m_6] \quad (28)$$

Nusselt Number :

The heat transfer rate in Nusselt is calculated by

$$N_u = \left(\frac{\partial \theta}{\partial y} \right)_{y=0} = \left(\frac{\partial \theta_0}{\partial y} \right)_{y=0} + E_c \left(\frac{\partial \theta_1}{\partial y} \right)_{y=0}$$

$$= -(b_1 m_1 + b_2 m_2) - E_c [2b_6 m_1 + 2b_7 m_2 + 2b_8 m_3 + b_9 (m_1 + m_2) + b_{10} (m_3 + m_2) + b_{11} (m_1 + m_3) + b_{12} m_5] \quad (29)$$

Sherwood Number :

The amount of mass transfer on the wall in Sherwood numbers

$$Sh = \left(\frac{\partial \phi}{\partial y} \right)_{y=0} = \left(\frac{\partial \phi_0}{\partial y} \right)_{y=0} + \left(\frac{\partial \phi_1}{\partial y} \right)_{y=0}$$

$$= -(m_1) \quad (30)$$

4. RESULTS AND DISCUSSION

For computations, the following default parameter values are used in this study: Gr=5.0, $\alpha=30$, $\alpha=30$, Gm 5.0, Ko=1.0, M=1.0, Pr=0.71, Ec=0.001, Q=0.1, Sc=0.6, Kr=0.1, R=0.5. Therefore, all graphs conform to these values, unless explicitly stated in $\frac{\pi}{6}, \frac{\pi}{4}, \frac{\pi}{3}$

Velocity Profiles:

Figure 2 indicates the α -inclined angle impact on the velocity profile. We observed the velocity reducing to the inclined angle α values. Figure 3 demonstrates the effects on velocity profile of aligned magnetic field parameter π . We found that the velocity declines as the aligned magnetic field parameter π rises. Figure 4 shows the influence of thermal Grashof number Gr on velocity.

This figure indicates that fluid velocity increases as Gr rises. This is attributed to a buoyancy impact that improves momentum. Figure 5 shows magnetic field influence in velocity spread. The existence of transverse magnetic field renders the fluid flow resistive. This force is called the Lorentz force, which slows down the fluid flow. Figure 6 displays the velocity profiles against the span-wise coordinate in the presence of the permeability parameter. We note that velocity decreases as parameter Ko. Figure 7 displays velocity profiles against changed Grashof number.

We note speed changes as changed Grashof number Gm changes. Figure 8 elucidates the influence of velocity profiles on various chemical reaction parameter (Kr) values. Figure 9

indicates that pace rises as Schmidt number Sc rises. Figure 10 demonstrates the influence of Radiation absorption parameter R on velocity distribution; from this figure, we found that the velocity increases with rises of Radiation absorption parameter. In Figure 11, reversal activity is observed to raise Prandtl number Pr .

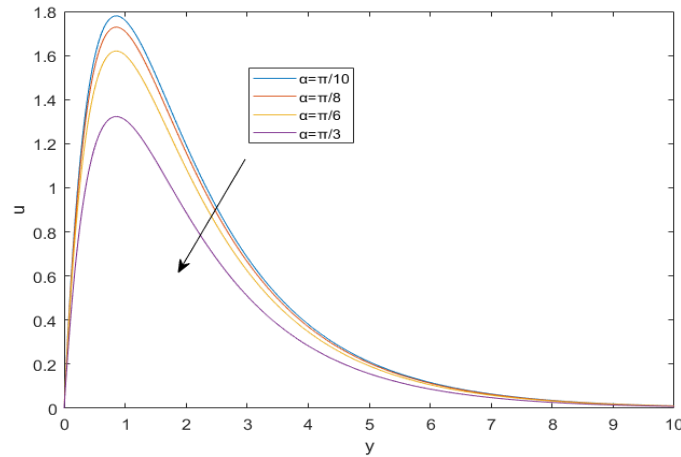


Fig 2: Velocity profiles for different values of α . $R=0.5$, $\gamma = \pi/6$, $Sc=0.6$, $Pr=0.71$, $Gr=5$, $Ko=1$, $Kr=0.1$, $M=1$, $Q=0.1$, $R=1$, $Gm=5$, $Ec=0.001$

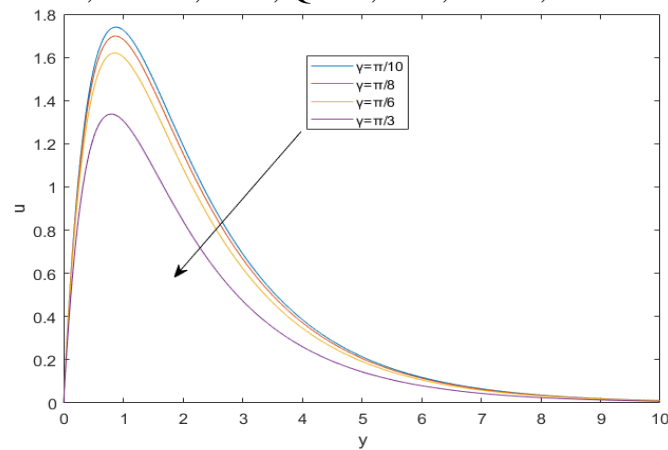


Fig 3: Velocity profiles for different values of α . $R=0.5$, $\alpha = \pi/6$, $Sc=0.6$, $Pr=0.71$, $Gr=5$, $Ko=1$, $Kr=0.1$, $M=1$, $Q=0.1$, $R=1$, $Gm=5$, $Ec=0.001$

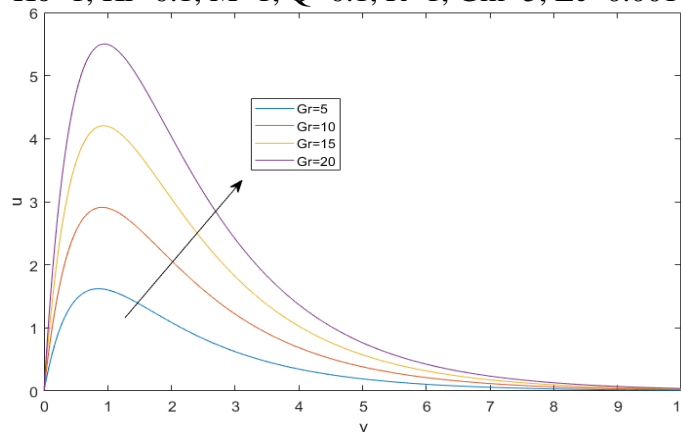


Fig 4: Velocity profiles for different values of Gr . $R=0.5$, $Sc=0.6$, $Pr=0.71$, $Ko=1$, $\gamma=30$, $\alpha=30$, $Kr=0.1$, $M=1$, $Q=0.1$, $R=1$, $Gm=5$, $Ec=0.001$

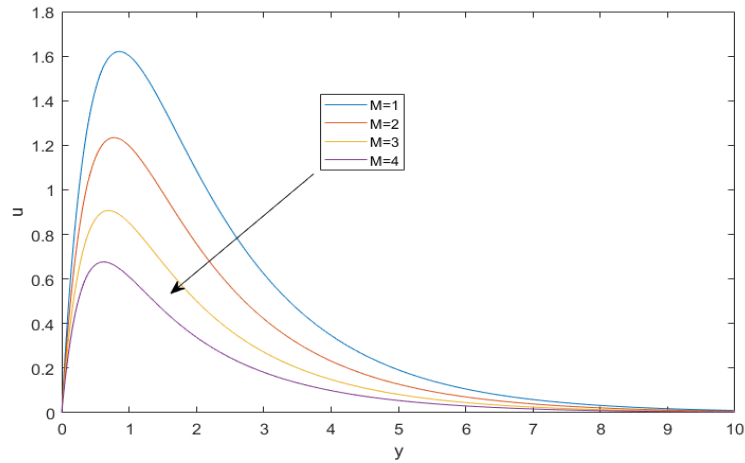


Fig 5: Velocity profiles for different values of M. $R=0.5$, $Sc=0.6$, $Pr=0.71$, $Ko=1$, $\gamma=30$, $\alpha=30$, $Kr=0.1$, $Gr=5$, $Q=0.1$, $R=1$, $Gm=5$, $Ec=0.001$

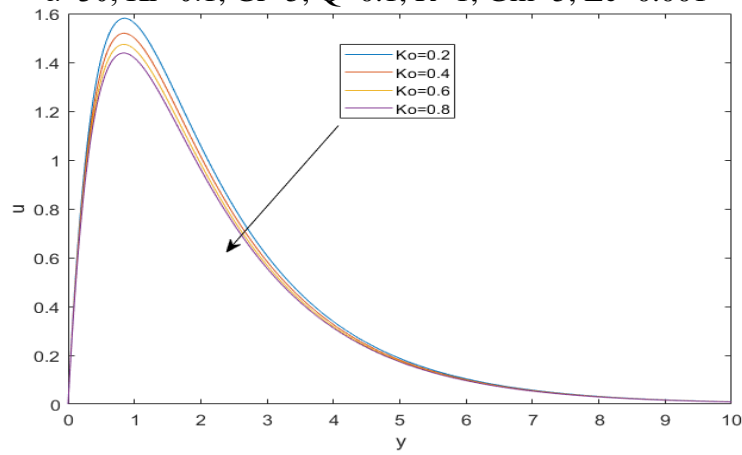


Fig 6: Velocity profiles for different values of Ko. $R=0.5$, $M=1$, $Sc=0.6$, $Pr=0.71$, $\alpha=30$, $Kr=0.1$, $\gamma=30$, $Gr=5$, $Q=0.1$, $R=1$, $Gm=5$, $Ec=0.001$

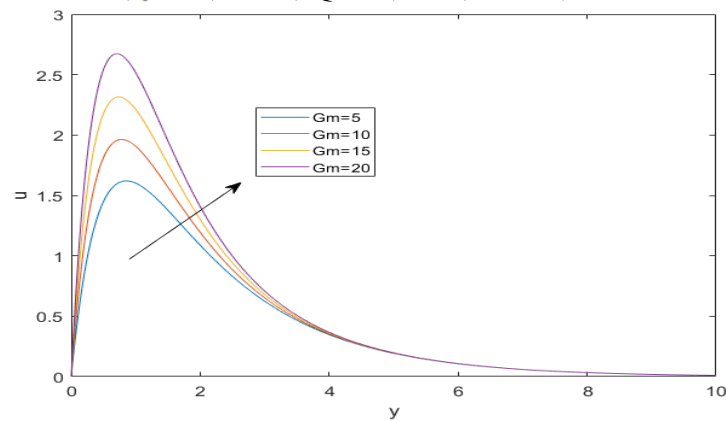


Fig 7: Velocity profiles for different values of Gm. $R=0.5$, $M=1$, $Sc=0.6$, $Pr=0.71$, $Ko=1$, $\alpha=30$, $\gamma=30$, $Kr=0.1$, $Gr=5$, $Q=0.1$, $R=1$, $Ec=0.001$

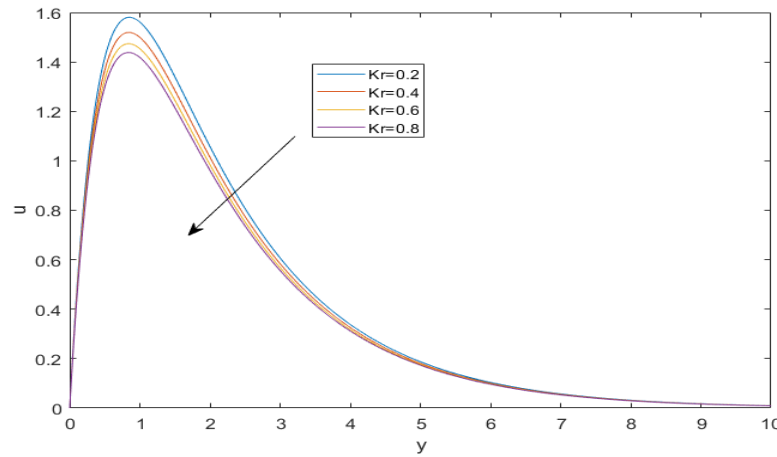


Fig 8: Velocity profiles for different values of Kr . $Q=0.5, M=1, Sc=0.6, Pr=0.71, Ko=1, \alpha=30, \gamma=30, Gr=5, Q=0.1, R=1, Gm=5, Ec=0.001$

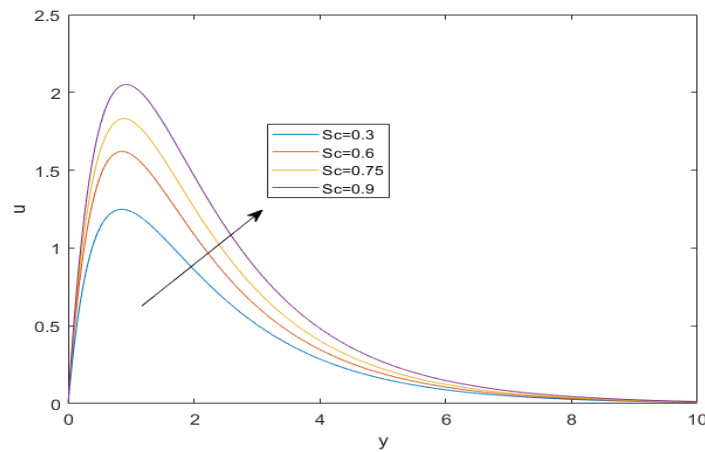


Fig 9: Velocity profiles for different values of Sc . $R=0.5, M=1, Pr=0.71, Ko=1, \alpha=30, \gamma=30, Kr=0.1, Gr=5, Q=0.1, R=1, Gm=5, Ec=0.001$

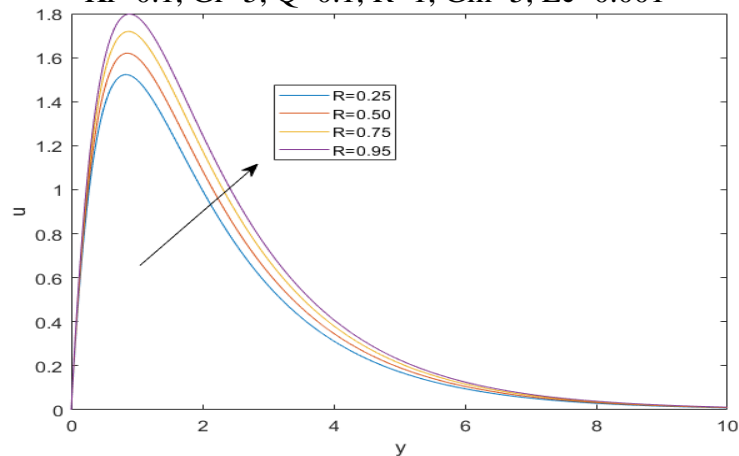


Fig 10: Velocity profiles for different values of R . $M=1, Sc=0.6, Pr=0.71, Ko=1, \alpha=30, \gamma=30, Kr=0.1, Gr=5, Q=0.1, R=1, Gm=5, Ec=0.001$

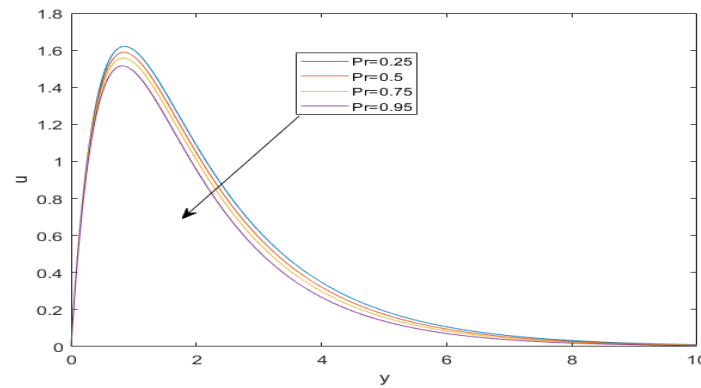


Fig 11: Velocity profiles for different values of Pr. $R=0.5, M=1, Sc=0.6, Pr=0.71, Ko=1, \alpha=30, \gamma=30, Kr=0.1, Gr=5, Q=0.1, R=1, Gm=5, Ec=0.001$

Temperature Profiles:

Figure 12 demonstrates the influence of heat source parameter Q on temperature distribution—the temperature declines as the heat source parameter Q rises. Figure 13 indicates that temperature declines as Prandtl rises. Figure 14 demonstrates the influence of Radiation absorption on temperature. Temperature is found to raise the Radiation absorption parameter R.

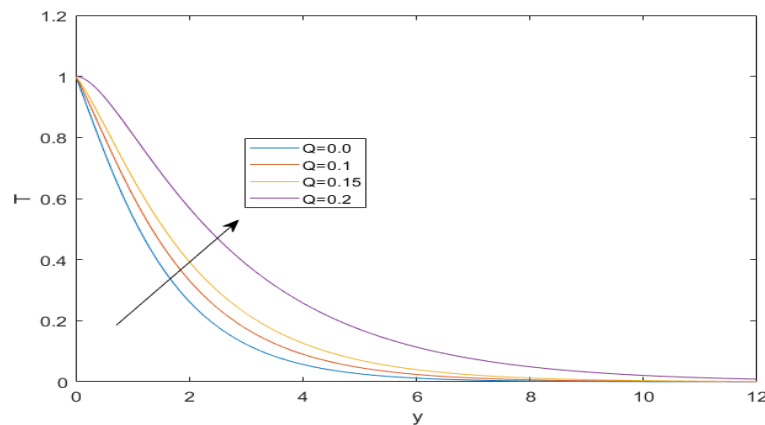


Fig 12: Temperature profiles for different values of Q. $R=0.5, M=1, Sc=0.6, Pr=0.71, Ko=1, \alpha=30, \gamma=30, Kr=0.1, Gr=5, R=1, Gm=5, Ec=0.001$

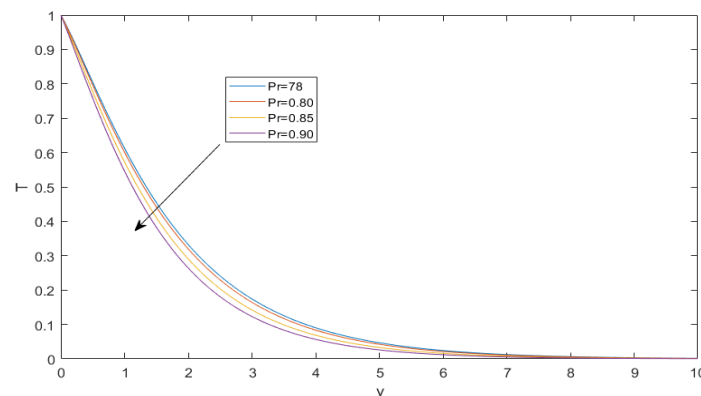


Fig 13: Temperature profiles for different values of Pr. $R=0.5, M=1, Sc=0.6, Q=0.1, Ko=1, \alpha=30, \gamma=30, Kr=0.1, Gr=5, R=1, Gm=5, Ec=0.001$

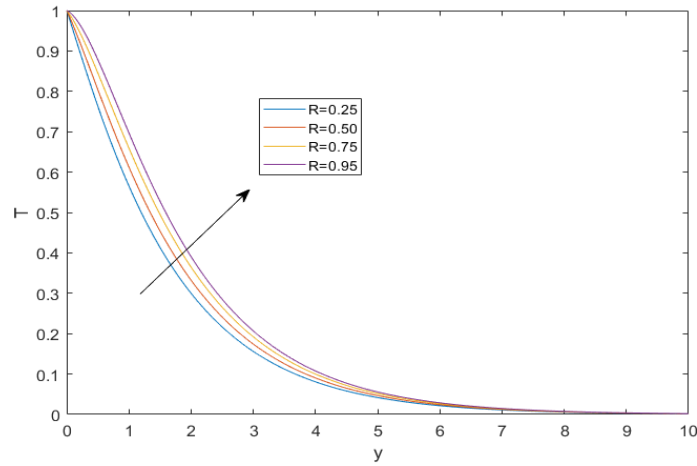


Fig 14: Temperature profiles for different values of R , $Q=0.5$, $M=1$, $Sc=0.6$, $Pr=0.71$, $Ko=1$, $\alpha=30$, $\gamma=30$, $Kr=0.1$, $Gr=5$, $R=1$, $Gm=5$, $Ec=0.001$

Concentration Profiles:

Figure 15 indicates that the concentration decreases with rising values of the Kr parameter chemical reaction. Figure 16 obvious that the layer thickness of the limit concentration decreases with Sc , and also that the concentration decreases exponentially and enters a free stream state for high Sc values.

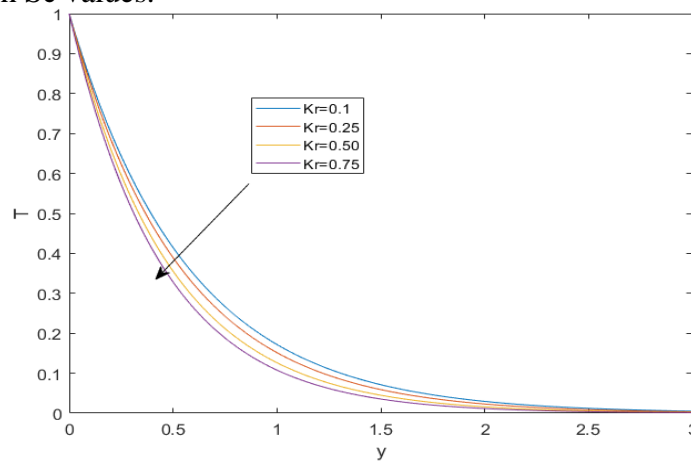


Fig 15: Concentration profiles for different values of Kr .

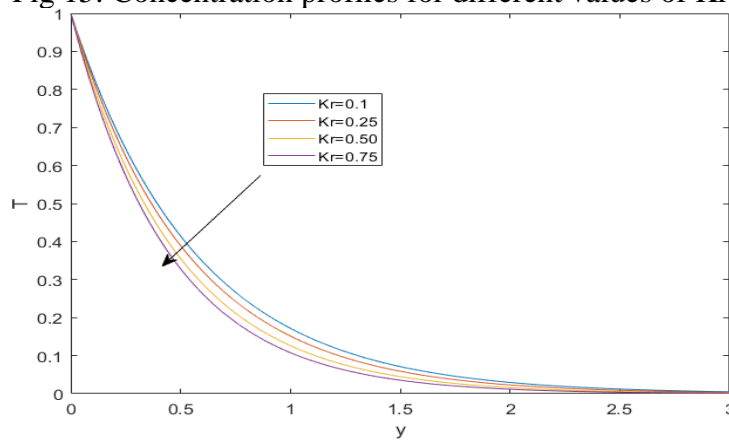


Fig 16: Concentration profiles for different values of Sc

Skin Friction (τ)

Gr	Gm	M	Ko	γ	α	Q	T
5							7.1611
10							10.6733
15							14.1925
	5						7.1611
	10						10.8155
	15						14.4673
		1.5					6.9677
		2					6.4417
		2.5					5.8393
			1				7.1611
			5				3.6578
			7.5				0.3186
				$\pi/10$			0.3187
				$\pi/6$			0.3186
				$\pi/3$			0.3185
					$\pi/10$		0.3499
					$\pi/6$		0.3186
					$\pi/3$		0.1840
						0.25	5.0642
						0.50	5.2755
						0.75	5.4549

Nusselt Number (Nu)

Pr	Ec	Q	R	Nu
0.75				-0.6312
0.80				-0.6828
0.85				-0.7342
	1			-0.5879
	5			-0.5810
	10			-0.5724
		0.1		-0.4717
		0.15		-0.5144
		0.20		-0.5366
			0.25	-7.0111
			0.50	-4.6990
			0.75	-2.8333

Sherwood Number (Sh)

Sc	Kr	Sh
0.6		-0.6145
1.2		-1.1013
1.8		-2.5014
	0.001	0.3581
	0.003	0.1430
	0.005	0.0052

Conclusion

The findings of this study are as follows.

1. Velocity decreases for increasing values of α , γ , M , K_r , K_o , R and Sc where as it shows reverse tendency in the case of Gr , G_m .
2. Temperature distribution decreases with an increase in Pr and (R) , where as it is enhances with increasing Q .
3. Concentration boundary layer decreases with an increase in K_r and Sc where as it is increases with increasing values of So .
4. skin-friction increases with an increase in (Gr) , (G_c) , (K_o) and (γ) , where as it decreases under the influence of (M) and (α) .
5. Nusselt number increases with an Ec , where as it decreases under the influence of (Pr) and (Q) .
6. Sherwood number increases with an increase in So but a reverse effect is noticed in the case of Sc and K_r .
- 7.

References

- [1]. S Mohammed Ibrahim , T Sankar Reddy , P. Roja, Radiation Effects on Unsteady MHD Free Convective Heat and Mass Transfer Flow Of Past a Vertical Porous Plate Embedded In a Porous Medium with Viscous Dissipation, International Journal of Innovative Research in Science, Engineering and Technology, Vol. 3, Issue 11, ISSN: 2319-8753
- [2]. K. Raghunath, Dr. R.Sivaprasad, & Dr. G.S.S. Raju., "Hall Effects on MHD Convective Rotating Flow of Through a Porous Medium past Infinite Vertical Plate" Published in Annals of Pure and Applied Mathematics, Vol. 16, No. 2, 2018, 353-263, ISSN: 2279-087X (P), 2279-0888(online), Published on 23rd February 2018, DOI <http://dx.doi.org/10.22457/apam.v16n2a12>.
- [3]. K. Raghunath, Dr. R.Siva Prasad, & Dr. G.S.S. Raju., "Heat and Mass Transfer on Unsteady MHD Flow of a Visco-Elastic Fluid Past an Infinite Vertical Oscillating Porous Plate", Published in British journal of Mathematics & Computer Science, volume17(6),July2016, ISSN:2231-0851,DOI:10.9734/BJMCS/2016/25872.
- [4]. G. Suresh Babu , G. Nagesh , K. Raghunath , Dr. R. Siva Prasad "Finite Element Analysis of Free Convection Heat Transfer Flow in a Vertical Conical Annular Porous Medium" Published in International Journal of Applied Engineering Research (Scopus), ISSN 0973-4562 Volume 14, Number 1 (2019) pp. 262-277.
- [5]. G.V Nagendra prasad , G. Nagesh , K. Raghunath , Dr. R. Siva Prasad "MHD flow of a Visco-elastic fluid over an unbounded rotating porous plate with Heat source and Chemical reaction" Published in International Journal of Applied Engineering Research (Scopus), ISSN 0973- 4562 Volume 13, Number 24 (2019) pp.16927-16938.
- [6]. Orthan A and Ahmet K, "MHD Mixed Convective Heat Transfer Flow about an Inclined Plate". Int.l Journal of Heat and Mass Transfer. Vol.46, (2009), 129-136.
- [7] Reddy, N.A, Varma, S.V.K., and Raju, M.C., "Thermo diffusion and chemical effects with simultaneous thermal and mass diffusion in MHD mixed convection flow with Ohmic heating", Journal of Naval Architecture and Marine Engineering, Vol. 6, No.2, 2009, 84-93.
- [8] Reddy, T.S., Raju, M.C., & Varma, S.V.K., "Unsteady MHD radiative and chemically reactive free convection flow near a moving vertical plate in porous medium", JAFM, Vol.6, no.3, pp. 443-451, 2013. International Journal of Engineering Research in Africa Vol. 20 159
- [9] Raju, K.V.S., Reddy, T.S., Raju, M.C, Satyanarayana, P.V., and Venkataramana, S., "MHD convective flow through porous medium in a horizontal channel with insulated and

impermeable bottom wall in the presence of viscous dissipation and Joule's heating", *Ain Shams's engineering Journal*, (2014), 5 (2), 543-551. DOI: 10.1016/j.asej.2013.10.007.

[10] Ravikumar, V., Raju, M.C., Raju, G.S.S., "Combined effects of heat absorption and MHD on convective Rivlin-Ericksen flow past a semi-infinite vertical porous plate", *Ain Shams Engineering Journal*, (2014) 5 (3), 867–875, DOI: 10.1016/j.asej.2013.12.014 ISSN: 2090- 4479.

[11] Raju, M.C., Reddy, N.A., Varma, S.V.K., "Analytical study of MHD free convective, dissipative boundary layer flow past a porous vertical surface in the presence of thermal radiation, chemical reaction and constant suction", *Ain Shams Engineering Journal*, Vol. 5 (4), 2014, 1361-1369. DOI: 10.1016/j.asej.2014.07.005.